THE IMPACT OF MITOCHONDRIAL MODULATION ON CARDIAC PERFORMANCE

Ph.D. Thesis

Author: Kitti Bruszt, M.D.

Program leader: Prof. Kálmán Tóth, M.D., Ph.D., D.Sc.

Project leaders: László Deres, Ph.D., Prof. Róbert Halmosi, MD., D.Sc.

1st Department of Medicine

University of Pécs, Medical School

Pécs, Hungary

2025

ABRREVIATIONS

ACE	Angiotensin-Converting Enzyme
ARB	Angiotensin II Receptor Blocker
ATP	Adenosine Triphosphate
BNIP3	BCL2/Adenovirus E1B 19 kDa-Interacting Protein 3
BNP	B-type Natriuretic Peptide
cAMP	Cyclic Adenosine Monophosphate
DNA	Deoxyribonucleic Acid
DRP1	Dynamin-Related Protein 1
E	Early Mitral Inflow Wave
E’	Early Diastolic Mitral Annular Velocity
EF%	Ejection Fraction (Percentage)
Fis1	Mitochondrial Fission Protein 1
GAPDH	Glyceraldehyde-3-Phosphate Dehydrogenase
GTP	Guanosine Triphosphate
JC-1	5,5′,6,6′-Tetrachloro-1,1′,3,3′-Tetraethylbenzimidazolyl-Carbocyanine Iodide
K	Potassium
L-OPA1	Long Isoform of Optic Atrophy Protein 1
LV	Left Ventricle
LVIDd	Left Ventricular Internal Diameter in Diastole
LVIDs	Left Ventricular Internal Diameter in Systole
LVEDV	Left Ventricular End-Diastolic Volume
LVESV	Left Ventricular End-Systolic Volume
MFF	Mitochondrial Fission Factor
Mfn1	Mitofusin 1
Mfn2	Mitofusin 2
MiD49	Mitochondrial Dynamics Protein 49
MiD51	Mitochondrial Dynamics Protein 51
mtDNA	Mitochondrial DNA
n	Sample Size
NMCM	Neonatal Mouse Cardiomyocyte
OCR	Oxygen Consumption Rate

OMA1	Overlapping with the m-AAA Protease 1 (Zinc Metalloprotease)
OPA1	Optic Atrophy Protein 1
PINK1	PTEN-Induced Kinase 1
PBS	Phosphate-Buffered Saline
S-OPA1	Short Isoform of Optic Atrophy Protein 1
TG	Transgenic
VDAC	Voltage-Dependent Anion Channel
WT	Wild Type
YME1L1	ATP-Dependent Zinc Metalloprotease YME1-Like 1
ΔΨ	Mitochondrial Membrane Potential

INTRODUCTION

The Significance and Management of Heart Failure

Heart failure imposes a substantial burden on healthcare systems worldwide, affecting nearly 40 million individuals. Among people over 70 years of age, approximately 10–15% suffer from this condition. Heart failure arises when the heart is unable to maintain adequate tissue perfusion despite normal filling pressures, or when sufficient oxygen delivery can only be achieved at the cost of elevated filling pressures. Chronic heart failure may decompensate easily, but acute heart failure can also occur in individuals without previous cardiac disease.

The evidence-based management of chronic heart failure aims to improve cardiac function, slow disease progression, and alleviate symptoms. Current pharmacological therapies primarily aim to reduce cardiac workload. Angiotensin-converting enzyme inhibitors (ACE-Is), angiotensin II receptor blockers (ARBs), and mineralocorticoid receptor antagonists modulate the renin-angiotensin-aldosterone system to lower blood pressure and enhance diuresis. Neprilysin inhibitors, when combined with ARBs, prevent the degradation of natriuretic peptides, thus promoting sodium and water excretion and reducing myocardial wall stress. Beta-blockers mitigate cardiac workload through their negative inotropic and chronotropic effects. Sodium-glucose co-transporter 2 (SGLT2) inhibitors, initially developed for diabetes, exert beneficial metabolic effects and induce osmotic diuresis, thereby reducing fluid retention.

In acute heart failure, vasodilators and diuretics form the basis of pharmacological treatment. In cases of hypotension, positive inotropic agents and vasopressors may be required to maintain cardiac output. While these agents may stabilize the patient in the short term, they increase myocardial oxygen demand, promote arrhythmogenesis, and may impair tissue oxygenation due to peripheral vasoconstriction—factors that may ultimately worsen long-term survival.

Despite advances in current treatment strategies that have improved both symptoms and survival, it is increasingly evident that targeted enhancement of cardiomyocyte energy metabolism—particularly mitochondrial function—could be essential in halting disease progression.

Mitochondrial Dynamics

Mitochondria are the primary source of energy production within cells. In adult myocardium, ATP is generated mainly via oxidative phosphorylation from the oxidation of reduced coenzymes derived

from fatty acid and, to a lesser extent, glucose metabolism. Due to its constant workload, the heart has the highest energy demand among all organs; mitochondria constitute 25–35% of cardiomyocyte volume to meet this demand. Beyond energy production, mitochondria also regulate calcium homeostasis, programmed cell death, reactive oxygen species (ROS) generation and detoxification, and several signaling pathways. In cardiomyocytes, mitochondria form a complex and dynamic network that adapts to cellular energy needs through continuous remodeling. This mitochondrial dynamics is governed by a balance between fusion and fission processes, which influence mitochondrial distribution, the removal of damaged regions, and apoptosis regulation. Overall, these dynamic processes are essential for maintaining cellular homeostasis and ensuring appropriate adaptation to physiological changes.

Mitochondrial fission is primarily regulated by the cytosolic dynamin-related GTPase protein DRP1. Upon activation, DRP1 translocates to the mitochondrial outer membrane, where it forms a ring-like structure that constricts and ultimately divides the organelle. Several outer membrane proteins, including MFF, MiD49, and MiD51, facilitate DRP1 recruitment and binding. Fis1, another outer membrane protein, modulates fission through alternative, indirect pathways.

Mitochondrial outer membrane fusion is mediated by mitofusin 1 (Mfn1) and mitofusin 2 (Mfn2), which form homo- and heterodimers to connect adjacent mitochondria. The inner membrane fusion is regulated by OPA1 (optic atrophy protein 1), a GTPase family member with multiple isoforms that differentially influence fusion and fission. The long isoform (L-OPA1) anchors to the inner mitochondrial membrane, supports membrane integrity, maintains cristae structure, and inhibits pore formation. Under stress conditions that reduce membrane potential, the mitochondrial metallopeptidase OMA1 cleaves L-OPA1 into the short isoform (S-OPA1), which inhibits fusion and promotes mitophagy by aiding in the elimination of damaged mitochondria. The ATP-dependent metalloprotease YME1L1 constitutively cleaves L-OPA1, finely tuning its activity and maintaining a balance between fusion and fragmentation, thereby stabilizing the mitochondrial network.

Damaged mitochondria are eliminated via mitophagy, which is essential for cellular health. This process is regulated by multiple signaing pathways, notably the PINK1-Parkin and BNIP3 pathways. Disruptions in fusion-fission dynamics or mitophagy impair mitochondrial function and contribute to the pathogenesis and progression of cardiovascular diseases such as ischemic heart disease, cardiomyopathies, and heart failure. Thus, targeting mitochondrial dynamics represents a promising novel therapeutic approach in the treatment of cardiovascular conditions.

In heart failure, the mitochondrial network within cardiomyocytes becomes disrupted, and dynamics shift toward fission. Excessive fission compromises inner mitochondrial membrane integrity, leading to a reduction in membrane potential ($\Delta\Psi m$). This results in impaired mitochondrial function, inadequate ATP production, decreased phosphocreatine/ATP ratios, dysfunction of the electron transport chain, increased ROS production, and elevated intracellular calcium levels.

Initial therapeutic strategies aimed to inhibit mitochondrial fission to preserve membrane potential and function. However, blocking fission also impeded mitophagy, leading to accumulation of dysfunctional mitochondria, which proved counterproductive in the long term. Consequently, under chronic stress conditions, promoting mitochondrial fusion and stabilizing membrane structure have emerged as preferable approaches.

Numerous genetically modified animal models have been developed to study the role of OPA1. Complete OPA1 knockout resulted in neonatal lethality in mice, leading researchers to develop an inducible OPA1 knock-out model, which exhibited signs of premature aging and death within three months of induction. X-chromosome–targeted Opa1 transgenesis allowed moderate OPA1 overexpression in all cells. These mice were viable and fertile with normal lifespan, and the mutation proved beneficial in certain mitochondrial disease models.

In our model, we used heterozygous knock-in mice expressing a mutant ΔS1 variant of the Opa1 gene in addition to the wild-type OPA1 protein. This mutant OPA1 isoform is resistant to cleavage by OMA1, which is typically activated under stress-induced reductions in mitochondrial membrane potential. The constitutively active YME1L1 cleavage at the S2 site remains unaffected by the mutation, ensuring sufficient production of functional S-OPA1 for normal fission signaling and chaperone activity.

Positive Inotropic Agents

Positive inotropic agents enhance myocardial contractility, increase cardiac output, and improve systemic circulation. Their long-term use is limited due to increased myocardial oxygen demand, the potential for tachycardia and malignant arrhythmias, and the risk of myocardial exhaustion. Particularly with sympathomimetics, increased mortality has been observed, restricting their use mainly to acute cardiogenic shock when systolic blood pressure remains below 90 mmHg despite adequate fluid resuscitation or when signs of hypoperfusion are present.

In the latter half of the 20th century, dopamine was widely used in acute heart failure. At low doses, it induces vasodilation via D1 receptor activation in the vascular wall, lowering blood pressure. At moderate doses, it stimulates β1-adrenergic receptors in the heart, producing positive inotropic and chronotropic effects. At high doses, it acts via α-adrenergic receptors, causing vasoconstriction and increasing blood pressure. With the advent of newer agents, dopamine use has declined and is no longer recommended in pure cardiogenic shock.

Dobutamine, a currently used synthetic catecholamine, primarily stimulates myocardial β1 receptors, increasing intracellular cAMP levels and calcium influx, thereby enhancing contractility. It also mildly stimulates β2 receptors, causing slight vasodilation and reducing peripheral resistance. Unlike dopamine, its minimal α1 activity helps avoid excessive vasoconstriction. Its use is limited by the risk of tachycardia, arrhythmias, and tolerance development.

Levosimendan, developed in the 1990s, binds to troponin C and enhances its calcium sensitivity, promoting actin-myosin interaction without increasing intracellular calcium or oxygen consumption. Additionally, it activates ATP-sensitive potassium channels in the vasculature, inducing vasodilation and reducing afterload. Mitochondrial K^+-channel activation may confer cytoprotective effects, contributing to its pleiotropic profile. Although rapidly metabolized, 5–10% is converted in the liver to the active metabolite OR-1896, which has a prolonged half-life (70–80 hours) and provides sustained inotropic and vasodilatory effects for several days post-administration. Its hypotensive effect limits its use.

Omecamtiv mecarbil is the first of a new generation of positive ionotropes, selectively activates cardiac myosin, stabilizing actin-myosin cross-bridges, thereby increasing systolic force and duration. Its mechanism is independent of intracellular cAMP or calcium, thus improving systolic function without elevating oxygen demand. In the GALACTIC-HF trial, it provided modest improvement in patients with significantly reduced ejection fraction, but no survival benefit was observed, and it did not receive regulatory approval. Prolonged systolic duration and resultant myocardial ischemia may underlie its potential adverse effects.

A more promising, experimental inotropic and lusitropic agent is istaroxime. It indirectly raises intracellular calcium by inhibiting Na^+/K^+-ATPase, enhancing contractility. Simultaneously, it stimulates the SERCA2a enzyme, improving calcium reuptake into the sarcoplasmic reticulum and supporting diastolic relaxation. Clinical studies demonstrated improvements in both systolic and diastolic function without increasing arrhythmia risk.

AIMS

In this study, we aimed to investigate the cardiac effects of the overexpressed OPA1 protein. To this end, we examined age-related changes in cardiac function in genetically modified mice overexpressing OPA1 using small-animal echocardiography. To elucidate the underlying mechanisms of functional alterations, we performed histological analyses, ultrastructural mapping of mitochondria, and quantification of proteins involved in mitochondrial dynamics. In addition, we sought to support our observations through the analysis of mitochondrial network architecture and functional characteristics.

A further objective of our work was to examine the effects of positive inotropic agents on mitochondrial function. Using H9C2 rat cardiomyoblast-derived cells, we assessed how dopamine, dobutamine, levosimendan, OR-1896, omecamtiv mecarbil, and istaroxime influence cell viability and mitochondrial respiratory efficiency. Furthermore, we aimed to evaluate the impact of levosimendan and its active metabolite OR-1896 on mitochondrial membrane potential. Based on the identified alterations, we sought to provide potential explanations for the paradoxical effects observed with positive inotropic agents.

METHODS

Animal Model

In our experiments, we utilized knock-in mice genetically engineered to express a mutant ΔS1 variant of the *Opa1* gene. The transgene was introduced into the murine genome using the PiggyBac transposon-based gene expression vector system. This mutant gene variant lacks the sequence encoding the S1 cleavage site, resulting in expression of a cleavage-resistant OPA1 isoform alongside the endogenous wild-type protein. To mitigate potential deleterious effects arising from excessive OPA1 activity, the colony was maintained in a heterozygous state. Transgenic animals were compared to their wild-type littermates, serving as controls.

Experiments were conducted on 11-week-old OPA1 transgenic mice (n=10) and wild-type controls (n=12). Echocardiography and blood pressure measurements were performed at 11 and 36 weeks of age. At the end of the experimental period, animals were sacrificed under inhalational anesthesia. Blood samples were collected directly from the heart for plasma BNP level determination via ELISA. The atria and great vessels were removed, and ventricular weight was recorded. The ventricles were either fixed in 6% formalin for histological examination or snap-frozen for subsequent Western blot analysis. Lung tissue was also frozen to assess the wet-to-dry lung weight ratio.

To evaluate interstitial collagen deposition, Masson's trichrome staining was employed. Cardiomyocyte cross-sectional diameter was measured using Picrosirius red staining to assess myocardial hypertrophy. Oxidative damage was evaluated via immunohistochemistry: protein oxidation was detected using a monoclonal anti-nitrotyrosine antibody, while DNA damage was assessed with an anti-8-oxoguanine antibody.

For ultrastructural analysis, the hearts of 36-week-old mice were retrogradely perfused through the aortic root, fixed, embedded, and sectioned using an ultramicrotome. Electron micrographs were captured at 12,000x and 25,000x magnification using a JEM 1200EX-II transmission electron microscope. Changes in the expression of proteins involved in mitochondrial dynamics were analyzed by Western blot. Mitochondrial DNA (mtDNA) copy number was determined from left ventricular wall samples using the GenElute™ Mammalian Genomic DNA Miniprep Kit.

Cell Model

Neonatal Cardiomyocyte Culture

Primary beating cardiomyocytes were isolated from 1–3-day-old neonatal OPA1 transgenic mice and their wild-type littermates. The cells were seeded at a density of 2×10^4 cells per well on 24-well glass-bottom plates or at 4×10^4 cells per well on XFp Miniplate plates. Cultures were maintained under sterile conditions at 37 °C in a humidified atmosphere containing 5% CO_2. The medium was replaced every 2–3 days.

Mitochondrial fragmentation was assessed using MitoTracker Red CMXRos staining and analyzed via fluorescence microscopy at 60× magnification. For detailed quantification of mitochondrial morphology, the ImageJ-based Mitochondrial Network Analysis (MiNA) plugin was used. Mitochondrial membrane potential was evaluated using JC-1 staining, and images were analyzed with ImageJ software. Cellular oxygen consumption rates were measured using the Agilent Seahorse XFp Extracellular Flux Analyzer, according to the manufacturer's protocol.

H9C2 Cell Culture

The H9C2 rat cardiomyoblast cell line was obtained from the European Collection of Cell Cultures (Salisbury, United Kingdom). Cells were cultured under sterile conditions at 37 °C in a humidified atmosphere with 5% CO_2 and were passaged at 1:3 ratios every 3–4 days upon reaching 70–80% confluency.

On the day of the experiment, cells were washed with PBS and then incubated for 2 hours at 37 °C in the presence of media containing the specified concentration of a given positive inotropic agent. Cell viability was assessed using the MTT assay. Mitochondrial function was evaluated using the Agilent Seahorse XFp Extracellular Flux Analyzer, while changes in mitochondrial membrane potential were analyzed via JC-1 staining.

Statistical Analysis

Statistical analysis was performed using SPSS for Windows, version 26.0. All data are expressed as the mean of repeated measurements ± standard error of the mean (SEM). Comparisons between two groups were made using the Student’s t-test. A p-value of <0.05 was considered statistically significant.

RESULTS

Impact of the OPA1 Transgenic Phenotype on Body Metrics, Systolic Blood Pressure, BNP Levels, and Echocardiographic Parameters

No statistically significant differences were observed in biometric parameters between the transgenic and wild-type groups, either at the beginning or at the end of the study period. Similarly, there were no significant differences in systolic blood pressure values or serum BNP concentrations between the two groups.

At the baseline, the left ventricular end-diastolic volume was significantly higher in the transgenic mice compared to their wild-type littermates ($p<0.05$; TG^{START} vs. WT^{START}). However, this difference was no longer detectable by the end of the study period (see Table 1). In 36-week-old transgenic mice, the ejection fraction showed a significant decrease compared to the initial value ($p<0.01$; TG^{END} vs. TG^{START}). In contrast, wild-type animals exhibited no statistically significant changes in systolic left ventricular function over time. Physiological parameter changes related to normal growth were not considered in the analysis.

Table 1. *Impact of the OPA1 Transgenic Phenotype on Echocardiographic Parameters During Aging.* LVIDd: left ventricular internal diameter at end-diastole; LVIDs: left ventricular internal diameter at end-systole; LVEDV: left ventricular end-diastolic volume; LVESV: left ventricular end-systolic volume; LV MASS: calculated left ventricular mass; EF: ejection fraction; E: peak mitral inflow velocity during early diastole; A: peak mitral inflow velocity during late diastole; E′: peak early diastolic mitral annular velocity. WT^{START}: wild-type littermates at 11 weeks of age; WT^{END}: wild-type littermates at 36 weeks of age; TG^{START}: OPA1 transgenic mice at 11 weeks of age; TG^{END}: OPA1 transgenic mice at 36 weeks of age. *p < 0.05 vs. WT_START, **p < 0.01 vs. TG_START. Values are presented as means ± SEM.

	WT^{START} (n=12)	**WT^{END} (n=12)**	**TG^{START} (n=10)**	**TG^{END} (n=10)**
LVIDd (mm)	4,07 ± 0,12	4,29 ± 0,11	4,35 ± 0.17	4,29 ± 0,17
LVIDs (mm)	2,99 ± 0,14	3,19 ± 0,18	3,02 ± 0,15	3,29 ± 0,19
LVEDV (µl)	65,82 ± 4,57	86,22 ± 5,17	89,03 ± 8,02*	90,58 ± 8,27
LVESV (µl)	30,95 ± 3,02	40,74 ± 4,38	37,49 ± 4,27	49,26 ± 6,86
LV MASS (mg)	110,97 ± 4,16	156,56 ± 10,39	136,94 ± 13,33	159,94 ± 15,62
EF (%)	57,23 ± 3,35	51,94 ± 3,04	58,6 ± 2,59	44,69 ± 3,56**
E/A	1,75 ± 0,08	2,48 ± 0,45	2,02 ± 0,13	2,03 ± 0,17
E/E'	30,21 ± 2,08	27,63 ± 2,65	28,69 ± 4,92	36,72 ± 4,93

Effect of Enhanced OPA1 Expression on Interstitial Collagen Deposition, Cardiomyocyte Diameter, and Protein and DNA Oxidation

To assess the extent of left ventricular fibrosis, Masson's trichrome staining was performed on cardiac samples from 36-week-old animals. As a positive control, heart tissue from 15-month-old wild-type mice was included. Both OPA1 transgenic and wild-type mice exhibited only minimal

interstitial collagen deposition, with no statistically significant difference between the two groups (WT: 12.99 ± 0.70% vs. TG: 11.92 ± 0.98%). To determine cardiomyocyte diameter, histological sections of the left ventricle from 36-week-old mice were stained with Picrosirius Red. Quantitative analysis revealed no significant difference in cardiomyocyte diameter between wild-type and transgenic animals (WT: 18.45 ± 0.18 μm vs. TG: 18.93 ± 0.5 μm). As markers of oxidative stress, immunohistochemical detection of nitrotyrosine and 8-oxoguanine formation was carried out on left ventricular sections from 36-week-old mice. Neither nitrotyrosine staining, indicative of oxidative protein damage (WT: 17.8 ± 2.7%, TG: 16.4 ± 1.4%), nor 8-oxoguanine staining, reflective of oxidative DNA damage (WT: 6.7 ± 0.4%, TG: 6.5 ± 0.5%), showed significant differences between the wild-type and OPA1 transgenic groups.

Ultrastructural Alterations Observed by Electron Microscopy

Longitudinal sections of myofibrils were evaluated to assess the status of the interfibrillar mitochondria by electron microscopy (Fig 1). The area of interfibrillar mitochondria was examine don electron micrographs (500 mitochondria/group were measured).

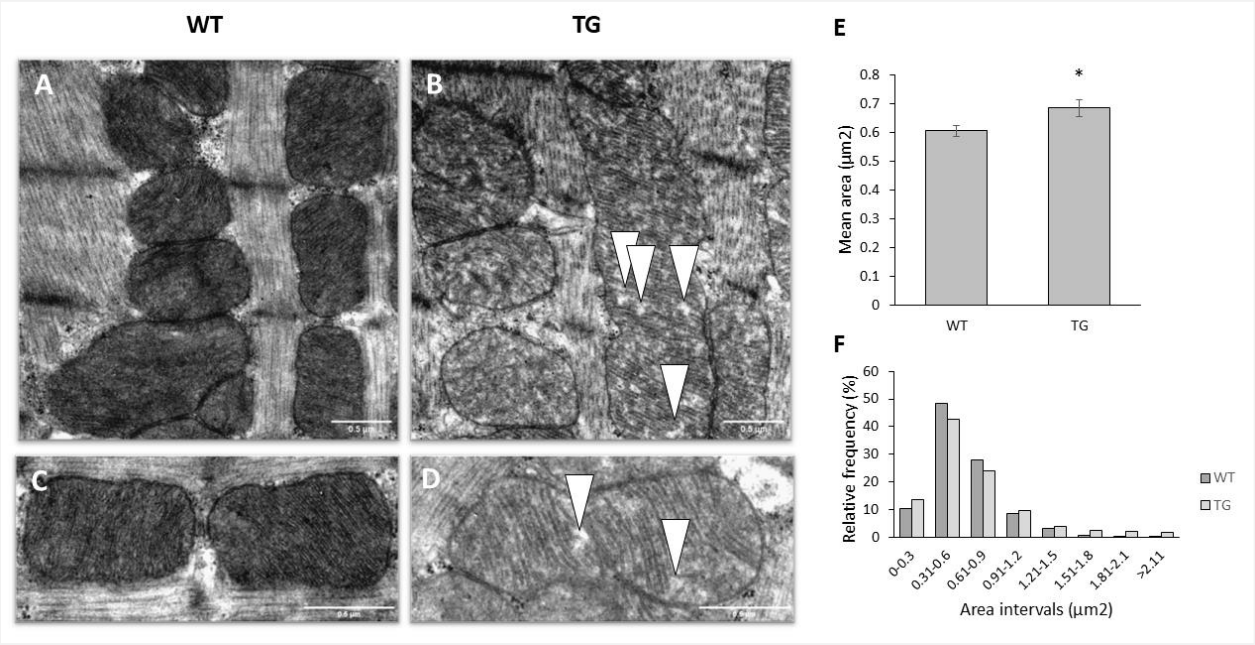

Figure 1. The Effect of Enhanced OPA1 Expression on Interfibrillar Cardiac Mitochondria at 36 Weeks of Age. Representative transmission electron micrographs of interfibrillar mitochondria in wild-type (A) and OPA1 transgenic (B) mice at 12,000× magnification (scale bar: 0.5 μm). Ultrastructural features of interfibrillar mitochondria in the myocardium of wild-type (C) and transgenic (D) animals at 25,000× magnification (scale bar: 0.5 μm). The relative frequency distribution of measured mitochondrial areas within defined intervals is shown in panel (F). WT: wild-type; TG: OPA1 transgenic mice. Data are expressed as mean ± SEM. *p < 0.05 vs. WT, n = 6.

We determined the relative frequencies of the measured mitochondrial areas in arbitrary intervals of 0.3 μm^2. In both groups, the predominant area range of the measured mitochondria was between 0.3 and 0.6 μm^2 (WT: 48.4% vs. TG: 42.8%). However, in the transgenic group, the size of the mitochondria was more heterogeneous. We found a higher proportion of mitochondria in both 0.9 μm^2 ranges (WT: 13.2% vs. TG: 19.6% than in the wild-type (Fig 1F). The mean mitochondrial area in transgenic animals was significantly larger than in wild-type (WT: 0.606 μm^2 vs. TG: 0.684 μm^2, $p<0.05$) Smaller vacuole-like intercristal widenings and a minor disruption of mitochondrial cristae structure could be observed in the transgenic group, moreover the mitochondrial matrix was also lighter (Fig 1D).

Morphological Changes in the Mitochondrial Network

We conducted a thorough quantification analysis of mitochondrial shapes using the Mitochondria Network Analysis tool (MiNA) on the ImageJ interface. The ultrastructurally observed larger mitochondrial area was not reflected in the characteristics of the mitochondrial network; the branch length of the mitochondrial network did not differ between the wild-type and transgenic animals.

Changes in Membrane Potential of Primary Cardiomyocytes Derived from OPA1 Transgenic Mice

We examined the mitochondrial membrane potential using JC-1, a cell-permeable voltage sensitive fluorescent mitochondrial dye (Fig 2). JC-1 emits red fluorescence if the mitochondrial membrane potential is high (aggregated dye), while depolarized mitochondria emit green fluorescence (monomer dye). We observed that the mitochondrial membrane potential was significantly different between the groups. Stronger green and weaker red fluorescence was detected in the transgenic NMCMs compared to the wild-type NMCMs.

Effect of OPA1 transgenic phenotype on mitochondrial oxygen consumption and energy metabolism in NMCM cells

Neonatal cardiomyocyte cells were isolated from transgenic animals and from their wild-type littermates. To determine the mitochondrial energy metabolism and respiratory function, we used the Agilent Seahorse XFp Analyser system and Agilent Seahorse XFp Cell Mito Stress test (Fig9).

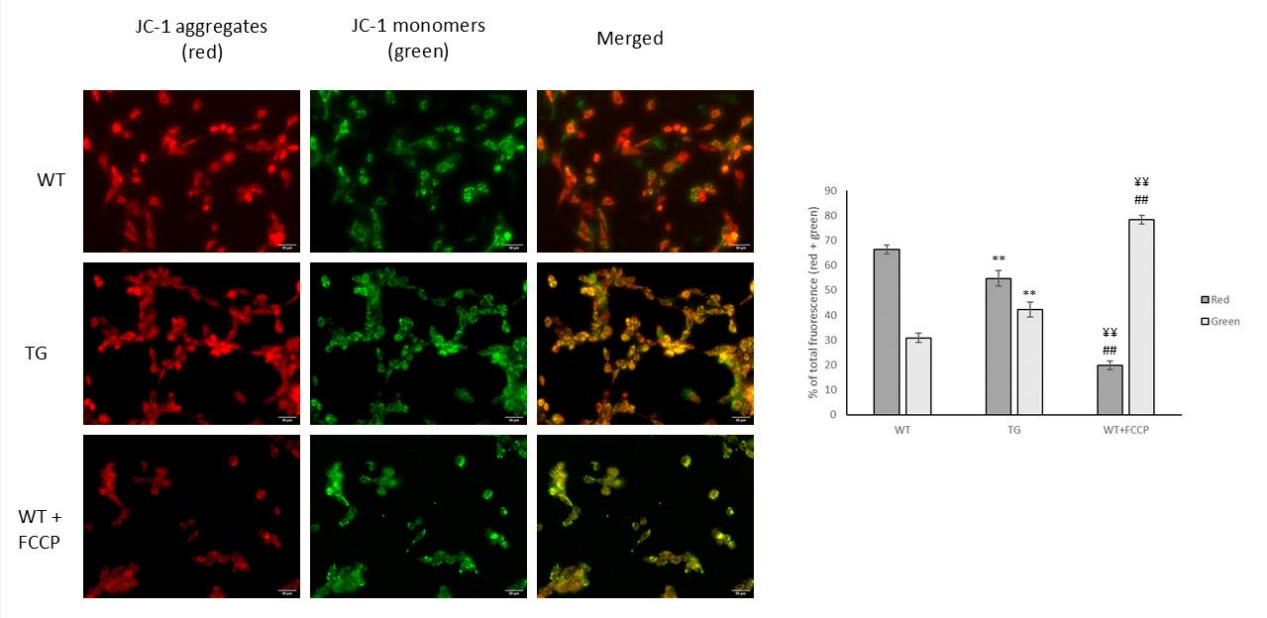

Figure 2. Effect of OPA1 transgenic phenotype on mitochondrial membrane potential in NMCM cells. Cells were stained with 5 µg/mL of JC-1, which is a membrane potential sensitive dye. The dye was loaded and after 90 minutes incubation, fluorescent microscopic images were taken using both the red and green channels. A: representative images are presented. Scale bar: 50 µm, magnification: 40-fold, WT: wild-type cardiomyocytes, TG: NMCM cells from OPA1transgenic mice. WT+FCCP: wild-type NMCM cells treated with 10 µM FCCP. B: quantitative analysis of mitochondrial polarization. Data are presented as the mean ± SEM of four independent measurements, n = 6. WT vs TG **p<0.01.

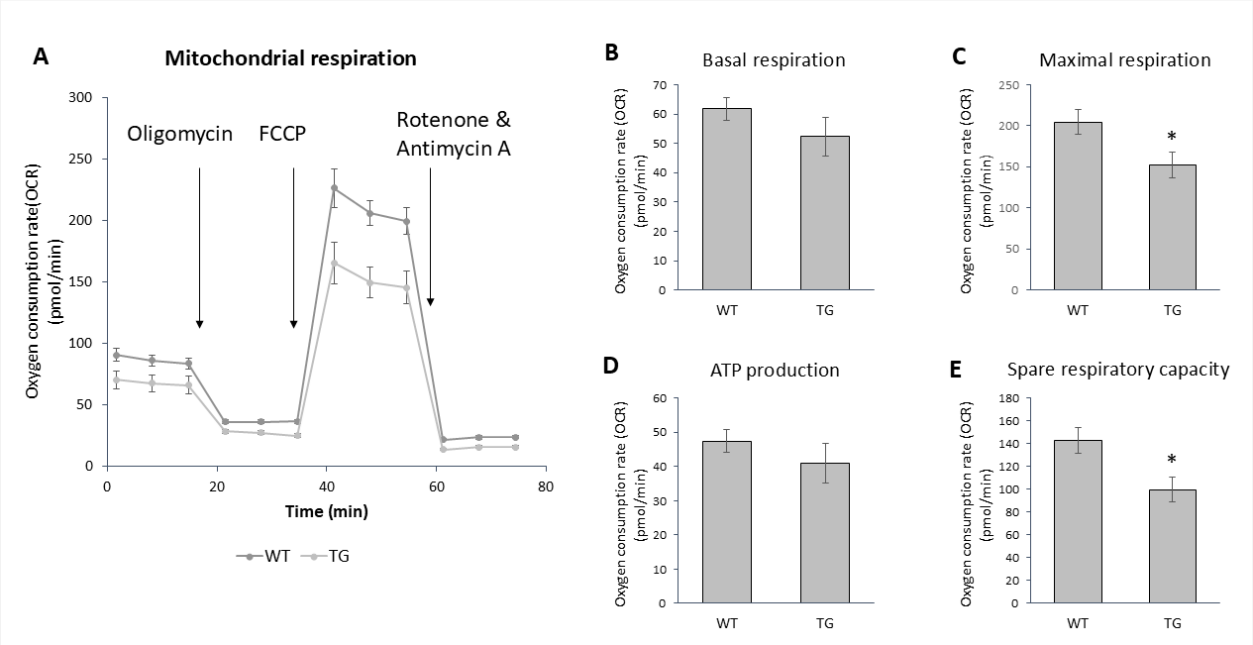

Figure 3. Changes in the oxygen consumption rate of OPA1 transgenic NMCM cells.A: oxygen consumption rate (OCR) in NMCM cells, measured by Seahorse XFp Analyser, B: basal respiration, C: maximal respiration, D: ATP production and E: spare respiratory capacity, WT: wild-type cardiomyocytes, TG: NMCM cells from OPA1 transgenic mice. *p<0.05 vs. WT. Values are means ±SEM, n=6

We observed that the oxygen consumption rate of the cells from the transgenic animals was lower compared to the wild-type cells. The deterioration was significant for maximal respiration (WT: 204.4 ± 15.05 pmol/min vs. TG: 152.21 ± 16.22 pmol/min, $p<0.05$) and spare respiratory capacity (WT: 142.7 ± 11.29 pmol/min vs. TG: 99.83 ± 10.89 pmol/min, $p<0.05$).

Effect of OPA1 transgenic phenotype on mtDNA copy number

To support the effect of OPA1 promotion more precisely on mitochondrial copy number, real-time PCR studies were performed. We found that the average number of mitochondrial copies was slightly increased in the TG group, but this increase did not reach statistical significance.

Effect of OPA1 transgenic phenotype on the proteins of the mitochondrial dynamics

The OPA1 level of transgenic animals was significantly increased compared to the wild-types ($p<0.01$ vs. WT group; Fig 4B).

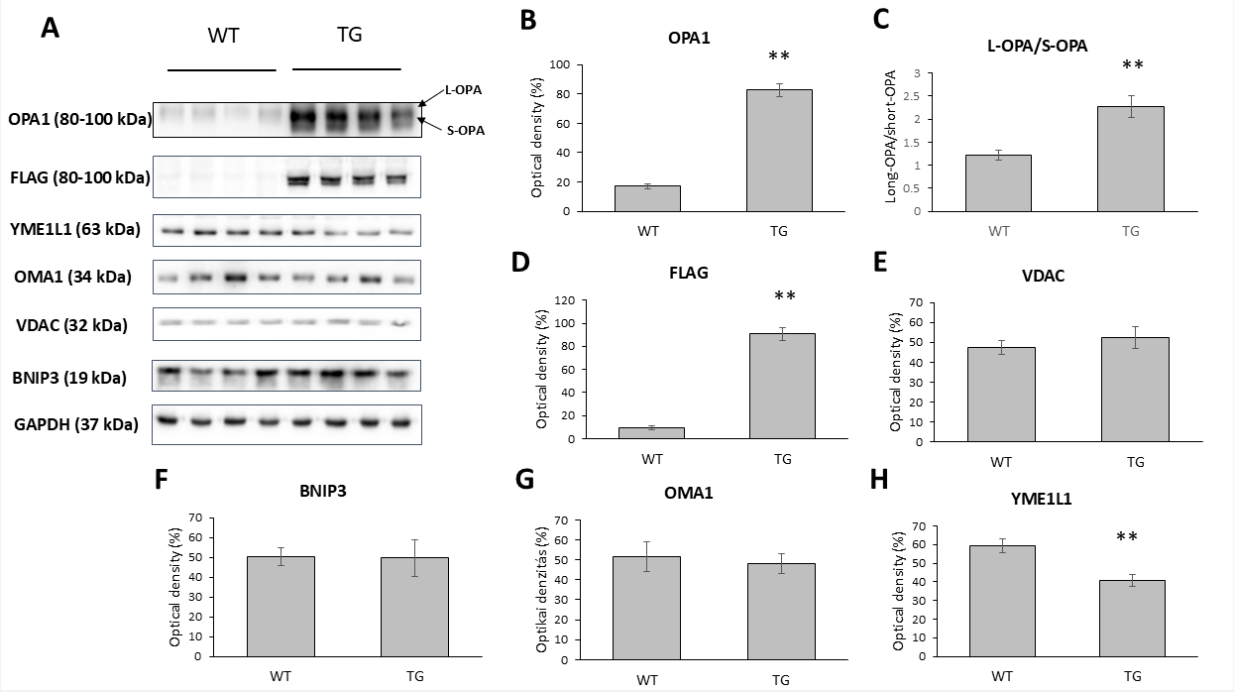

Fig 4. Changes of OPA1, OMA1 and YME1L1level. Representative Western blot analysis of OPA1, DYKDDDDK Tag (FLAG), VDAC, BNIP3, OMA1, YME1L1anddensitometric evaluation are shown. GAPDH was used as a loading control. WT: wild-type mice (n = 8), TG: OPA1 transgenic mice (n = 8). Values are mean ± SEM. ** $p < 0.01$ vs. WT.

In the transgenic group primarily the amount of short OPA1 increased, the L-OPA1/S-OPA1 ratio was significantly lower ($p < 0.01$ vs. WT group; Fig 4C). Transgenic origin of the elevated OPA1 level was demonstrated with using DYKDDDDK Tag (FLAG) antibody ($p< 0.01$ vs. WT group; Fig 4D). The amount of VDAC, indicating total mitochondrial mass, did not differ significantly between the two groups (Fig 4E). Levels of proapoptotic mitochondrial BNIP3 did not differ between groups (Fig 4F). The level of OMA1 protease was similar in the transgenic and wild type animals (Fig 4G), while the expression level of YME1L1 was significantly lower in the transgenic animals ($p < 0.01$ vs. WT group; Fig 4H).

There was no significant difference between the groups in the case of Mfn1, but Mfn2 showed a decreasing tendency in the transgenic animals (Fig 5B and 5C). There was no difference in the level of fission proteins DRP1 and Fis1 between the two groups (Fig 5D and 5E). The amount of PINK1 and Parkin proteins, which play a role in mitophagy, increased in the transgenic group, in the case of PINK1 the change was significant ($p < 0.05$; Fig 5F and 5G).

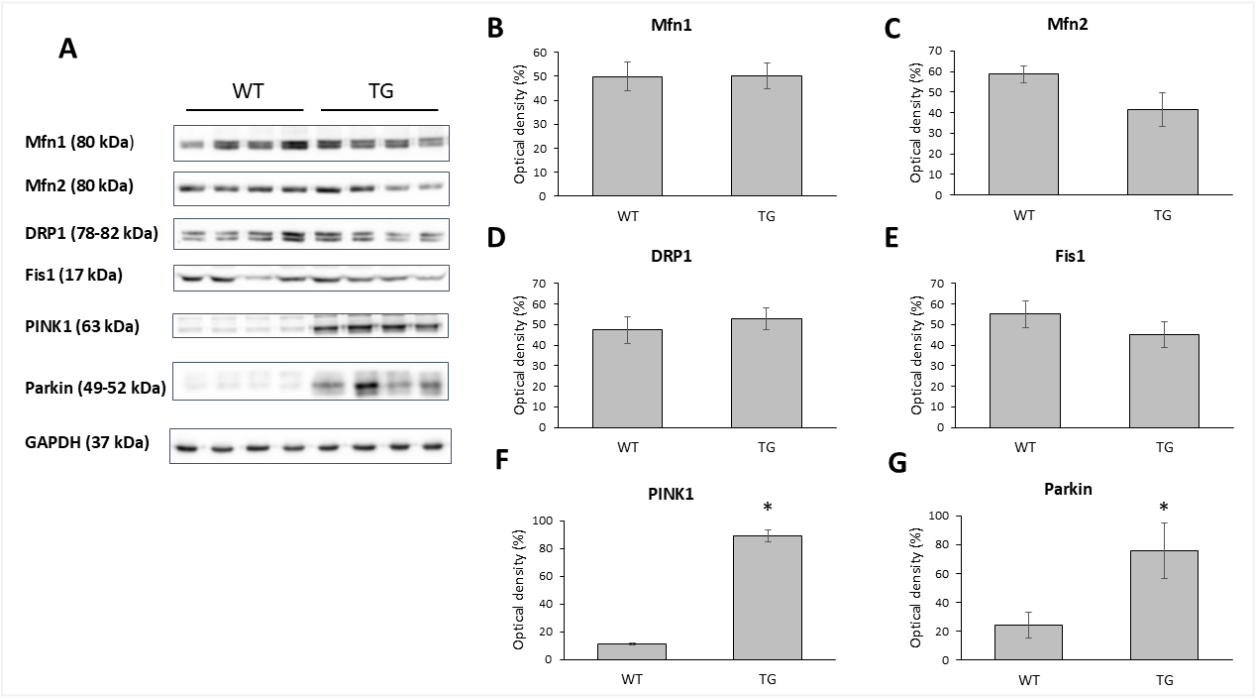

Fig 5. Changes in protein levels of mitochondrial dynamics. Representative Western blot analysis of Mfn1, Mfn2, DRP1, Fis1, PINK1, Parkin and densitometric evaluation are shown. GAPDH was used as a loading control. WT: wild-type mice (n = 8), TG: OPA1 transgenic mice (n = 8). Values are mean ± SEM.*$p<0.01$ vs. WT.

Effect of Positive Inotropic Agents on Cell Viability

H9C2 cardiomyoblast cultures were incubated for 2 hours with dopamine hydrochloride, dobutamine hydrochloride, levosimendan, OR-1896, omecamtiv mecarbil, and istaroxime hydrochloride at concentrations of 0.1, 0.5, 1, 5, 10, 50, 100, 500, and 1000 µmol/l. Cytotoxicity of the compounds was assessed using the MTT assay following the 2-hour incubation period. Dopamine, dobutamine, and levosimendan caused a measurable decrease in cell viability from 500 µmol/l, while omecamtiv mecarbil and istaroxime hydrochloride exhibited cytotoxic effects only at the highest concentration of 1 mmol/l. Notably, the active metabolite of levosimendan, OR-1896, did not induce any detectable reduction in cell number at any tested concentration, including 1 mmol/l, compared to control.

Effect of Positive Inotropic Agents on Mitochondrial Respiratory Efficiency

The effects of dopamine hydrochloride, dobutamine hydrochloride, omecamtiv mecarbil, and istaroxime were evaluated at concentrations of 0.1, 1, 10, 100, and 1000 µmol/l, while levosimendan and its active metabolite OR-1896 were tested at 1, 10, and 100 nmol/l as well as 1 and 10 µmol/l using the Agilent Seahorse XFp Analyzer and the Seahorse XF Cell Mito Stress Test assay. Dopamine had no significant effect on cellular respiration at any tested concentration. In contrast, dobutamine consistently suppressed oxygen consumption across all concentrations, with statistically significant reductions observed from 1 µmol/l in basal respiration and from 100 µmol/l in ATP production (Figure 6).

Levosimendan decreased oxygen consumption at 10 nmol/l, 100 nmol/l, and 1 µmol/l; this reduction was significant at 100 nmol/l for maximal respiration and spare respiratory capacity, while lower concentrations showed only a non-significant decreasing trend. OR-1896 increased oxygen consumption significantly at 1 nmol/l, particularly in terms of maximal respiration; however, at 100 nmol/l and 1 µmol/l, a declining trend was observed in both maximal respiration and spare capacity. At the highest tested concentration (10 µmol/l), both levosimendan and OR-1896 yielded values similar to those of the control (Figure 7).

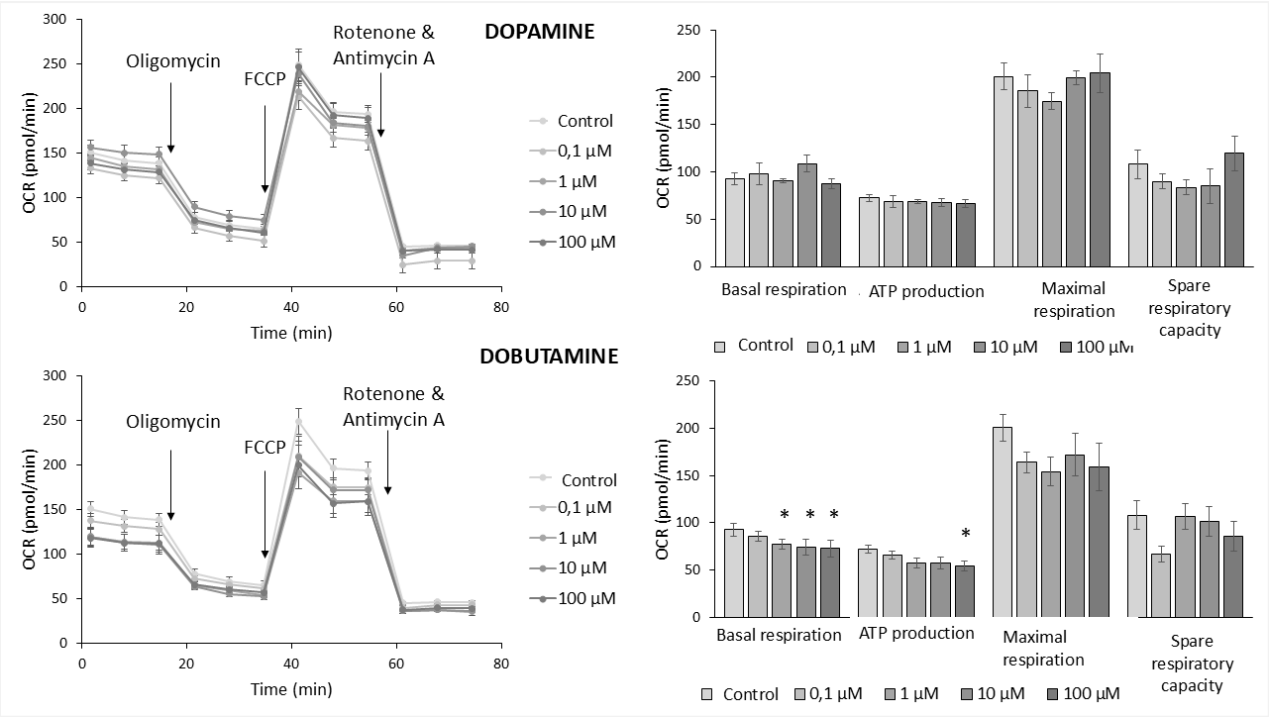

Figure 6. Effects of Dopamine and Dobutamine on Mitochondrial Oxygen Consumption. Following a 2-hour treatment, H9C2 cells were sequentially exposed to 10 µM oligomycin, 10 µM FCCP, and 5 µM rotenone/antimycin A. Data were analyzed using the Agilent Seahorse XF Cell Mito Stress Test Report Generator. OCR: oxygen consumption rate. Values are expressed as mean ± SEM (n=6). *p<0.05 vs. control.

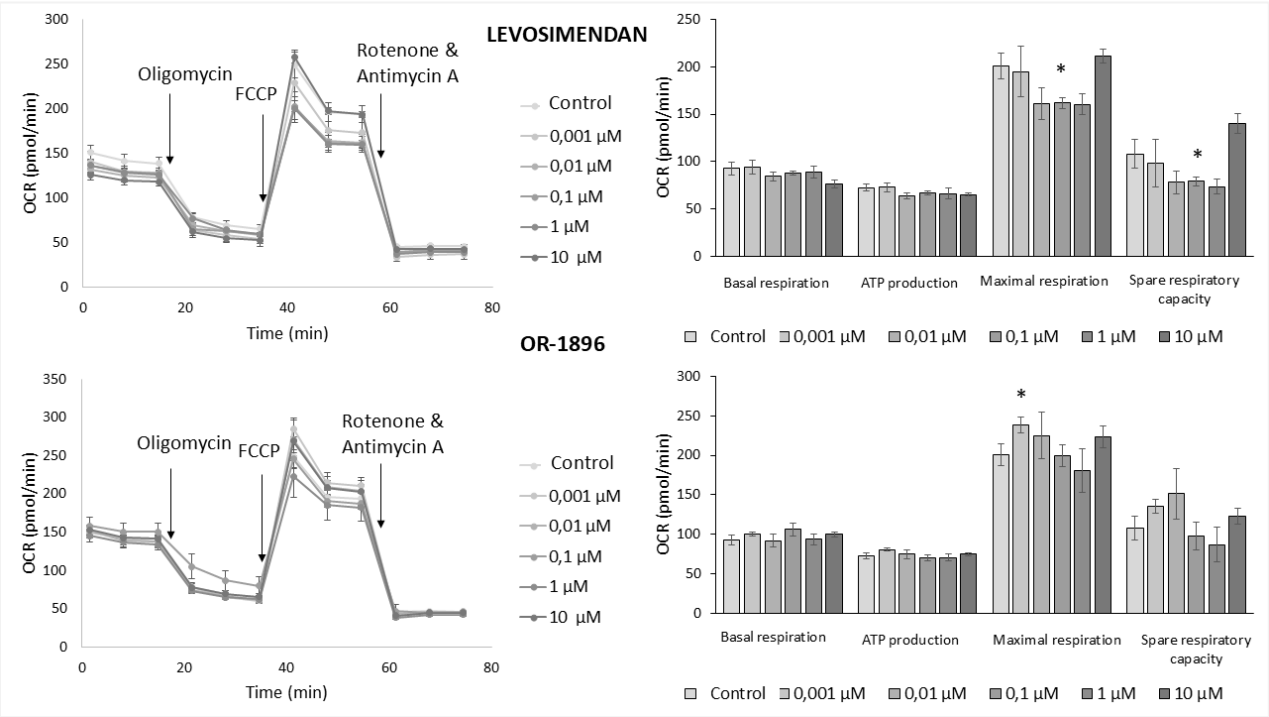

Figure 7. Effects of Levosimendan and OR-1896 on Mitochondrial Respiration. H9C2 cells were treated for 2 hours, followed by assessment of mitochondrial oxygen consumption using the Seahorse XFp analyzer. Basal respiration, ATP production, maximal respiration, and spare respiratory capacity were calculated using the Agilent Seahorse XF Cell Mito Stress Test Report Generator. OCR: oxygen consumption rate. Data are presented as mean ± SEM (n=6). *p<0.05 vs. control.

Omecamtiv mecarbil did not cause marked changes in mitochondrial respiration. Istaroxime at low concentrations (0.1 µmol/l) significantly enhanced oxygen consumption, especially regarding maximal respiration and spare capacity. At higher concentrations (10 and 100 µmol/l), however, it impaired mitochondrial respiration, with statistically significant reductions observed in ATP production, maximal respiration, and spare respiratory capacity (Figure 8).

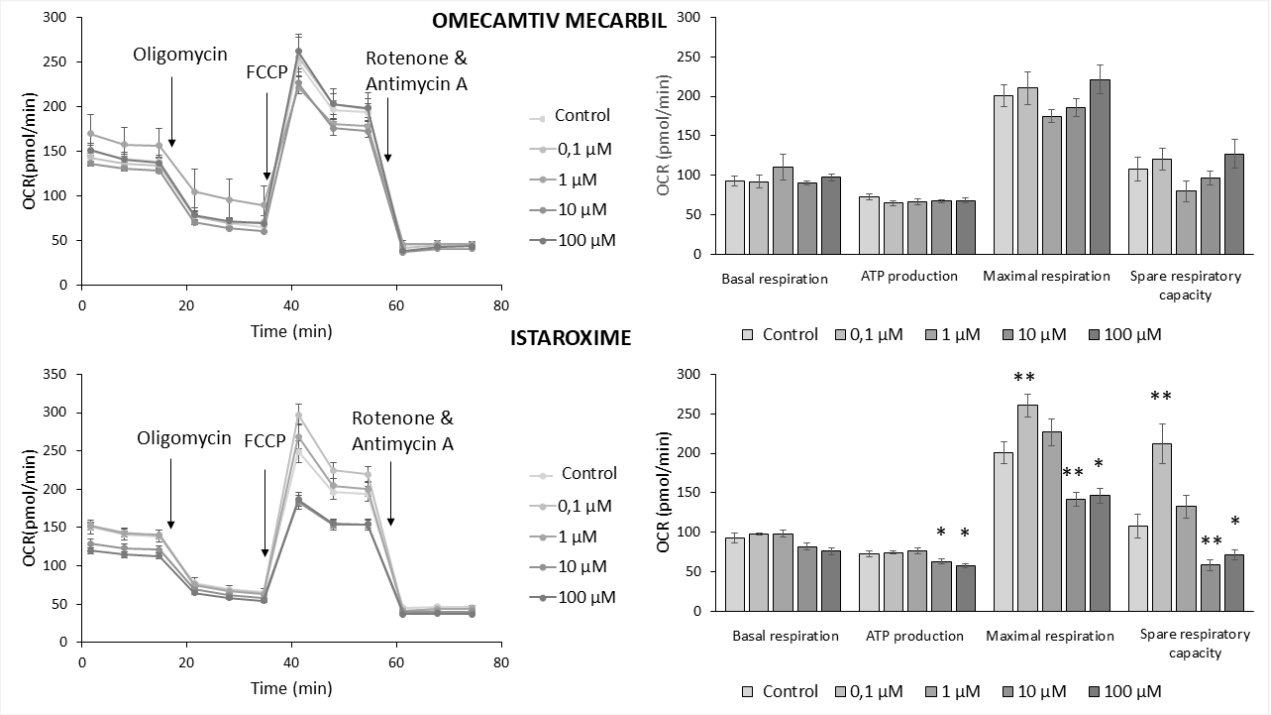

Figure 8. Effects of Omecamtiv Mecarbil and Istaroxime on Mitochondrial Energy Metabolism. Following 2-hour treatment, H9C2 cells were analyzed using the Seahorse XFp analyzer. Changes in oxygen consumption upon the addition of oligomycin, FCCP, and rotenone/antimycin A were used to calculate basal respiration, ATP production, maximal respiration, and spare respiratory capacity with the Agilent Seahorse XF Cell Mito Stress Test Report Generator. OCR: oxygen consumption rate. Data are presented as mean ± SEM (n=6). *p<0.05 vs. control, **p<0.01 vs. control.

Effect of Levosimendan and OR-1896 on Mitochondrial Membrane Potential

To assess the impact of levosimendan and its active metabolite OR-1896 on mitochondrial membrane potential, JC-1 fluorescent dye staining was performed. In cells treated with levosimendan, an increased proportion of green fluorescent monomers were observed across all tested concentrations, indicating a reduction in mitochondrial membrane potential. However, this alteration reached statistical significance only at the lowest concentration tested (0.001 µM; $p<0.05$ vs. control). In contrast, no significant changes in mitochondrial membrane potential were detected in response to OR-1896 at any concentration examined.

CONCLUSION

It is well established that the development of heart failure is accompanied by both morphological and functional alterations of mitochondria. Mitochondrial dynamics shift toward fragmentation, leading to the disintegration of the network structure, accompanied by a decline in membrane potential—processes that may contribute to the mitochondrial dysfunction observed in heart failure. Strengthening mitochondrial fusion and stabilizing membrane architecture may thus represent promising therapeutic targets.

In our investigations, we used a transgenic mouse line that expresses, in addition to the wild-type protein, a variant of OPA1 lacking the OMA1 cleavage site, resulting in a marked increase in total OPA1 expression. Cardiac function in these animals was monitored by small-animal echocardiography, and aging was associated with a significant decrease in ejection fraction in transgenic mice. The deterioration in systolic function was not accompanied by fibrotic remodeling or changes in cardiomyocyte diameter, nor did BNP levels or lung wet-to-dry ratio indicate overt heart failure.

Mitochondrial network analysis did not reveal significant changes in average mitochondrial size, but ultrastructural evaluation demonstrated a heterogeneous size distribution, mildly distorted cristae architecture, and reduced matrix electron density. In cardiomyocytes isolated from neonatal mice, a reduction in mitochondrial membrane potential and impaired energy metabolism were also evident. Protein analysis showed an increase in both L-OPA1 and S-OPA1 isoforms, with a shift in the ratio favoring L-OPA1. The transgenic origin of the expressed protein was confirmed by FLAG-tag detection. Normal VDAC expression and unchanged mitochondrial DNA copy number confirmed that the observed effects were not due to increased mitochondrial mass.

While the amount of OMA1 protease remained unchanged, levels of the constitutively expressed YME1L1 were significantly decreased, suggesting a disruption in proteolytic balance. Additionally, upregulation of the mitophagy regulators PINK1 and Parkin indicated enhanced clearance of damaged mitochondria, whereas low BNIP3 levels did not support activation of overt mitophagy or proteasomal degradation.

Although we initially hypothesized a protective effect of OPA1 overexpression, we instead observed a deterioration in cardiac function. This may be explained by excessive incorporation of L-OPA1 into the mitochondrial membrane, disruption of the fusion–fission balance, and subsequent impairment of mitochondrial function.

Our interest in the mitochondrial effects of positive inotropic agents was driven by the clinical observation that although traditional inotropes such as dobutamine and dopamine improve cardiac output in the short term, they paradoxically worsen survival over the long term—a phenomenon potentially linked to mitochondrial effects.

In our experiments, dobutamine reduced basal respiration and, at higher concentrations, also inhibited ATP production. In contrast, dopamine did not exert such effects, which may be attributed to differences in receptor targeting. The calcium-sensitizer levosimendan also impaired mitochondrial function, reducing maximal and spare respiratory capacity, and caused a drop in membrane potential even at low concentrations.

However, its active metabolite, OR-1896, enhanced maximal respiration at low doses without affecting mitochondrial membrane potential—likely due to its distinct pharmacokinetic profile and prolonged action.

The first-in-class myosin activator omecamtiv mecarbil enhances contractility without significantly altering calcium homeostasis or increasing oxygen demand. Our findings confirmed that it does not have a significant impact on mitochondrial function.

In contrast, istaroxime, which has shown clinical promise, improved respiratory parameters at low doses but exhibited detrimental effects at higher concentrations, decreasing ATP production. This dose-dependent duality suggests that istaroxime may exert direct mitochondrial effects beyond its known actions on Na^+/K^+-ATPase inhibition and SERCA2a activation.

In summary, our results suggest that the adverse effects of positive inotropic agents on survival may, in part, be due to their influence on mitochondrial function. These novel findings could inform the optimization of inotropic therapy and contribute to improved treatment strategies for heart failure.

RESULTS AND OBSERVATIONS

1. We observed that systolic cardiac function declined with age in transgenic mice overexpressing the OPA1 protein compared to their wild-type littermates.
2. We confirmed that OPA1 overexpression induced ultrastructural changes in mitochondria, characterized by vacuole-like widening of the intercristae space and, in some regions, disruption of cristae architecture. Despite the high levels of OPA1 protein, the average mitochondrial size showed only a slight increase.
3. Mitochondrial function in cardiomyocytes isolated from OPA1-overexpressing mice was impaired compared to cells from wild-type littermates. This was demonstrated by reduced maximal and spare respiratory capacity using the Agilent Seahorse platform, and by decreased mitochondrial membrane potential as detected by JC-1 staining.
4. OPA1 overexpression resulted in an altered OMA1/YME1L1 ratio due to a significant decrease in YME1L1 levels and was associated with increased expression of the mitophagy-related proteins PINK1 and Parkin.
5. We confirmed that dobutamine reduced basal mitochondrial respiration in H9C2 cells in a dose-dependent manner, while dopamine had no significant effect on mitochondrial function.
6. Levosimendan impaired mitochondrial function in cultured cells, significantly reducing both maximal and spare respiratory capacity. This was accompanied by a decrease in mitochondrial membrane potential. In contrast, its active metabolite OR-1896 enhanced maximal respiration at low concentrations without significantly affecting membrane potential.
7. Seahorse analysis demonstrated that omecamtiv mecarbil did not significantly influence mitochondrial function.
8. Istaroxime improved mitochondrial function at low concentrations in H9C2 cell cultures but impaired it at higher doses.

ACKNOWLEDGEMENTS

Our experiments were conducted at the University of Pécs, within the János Szentágothai Research Centre and the Institute of Biochemistry and Medical Chemistry at the Medical School of the University of Pécs between 2019 and 2024.

I would like to express my sincere gratitude to my program leader, Professor Kálmán Tóth, for providing me the opportunity to carry out my work. I am deeply thankful to my supervisors, Professor Róbert Halmosi and László Deres, for their support and patience, which greatly contributed to fostering my commitment to the subject. I am also grateful to my colleagues, Orsolya Horváth, Katalin Ördög, Tímea Völgyiné Dózsa, and Szilárd Tóth, for their indispensable practical assistance during my research and experiments.

Special thanks go to Professor Ferenc Gallyas for enabling us to perform most of the experiments at the Institute of Biochemistry and Medical Chemistry, as well as to the staff of the Biochemistry Institute for their help in my work: Kata Juhász and Eszter Vámos for their assistance in cell-based studies, and Katalin Fekete, Gergő Bárándi, and Mária Horváthné Szegedi for their support with animal experiments.

Furthermore, I wish to thank Professor László Seress, Béla Kajtár, and József Nyirádi for their expert contributions to the preparation of electron microscopy and histological images. Finally, I am especially grateful to my family for supporting my studies and for their patience during the challenging times.

PUBLICATIONS OF THE AUTHOR

Relevant publications

BRUSZT K, HORVATH O, ORDOG K, TOTH SZ, JUHASZ K, VAMOS E, FEKETE K, GALLYAS F, TOTH K, HALMOSI R, DERES L. Cardiac effects of OPA1 protein promotion in a transgenic animal model. PLOS ONE 10.1371/journal.pone.0310394 (2024)
Q1, IF: 2,9

Additional publications

HORVATH O, ORDOG K, **BRUSZT K**, DERES L, GALLYAS F, SUMEGI B, TOTH K, HALMOSI R. BGP-15 protects against heart failure by enhanced mitochondrial biogenesis and decreased fibrotic remodelling in spontaneously hypertensive rats. Oxidative Medicine and Cellular Longevity 2021 Paper: 1250858, 13 p. (2021)
Q1, IF: 7,31

ORDOG K, HORVATH O, EROS K, **BRUSZT K**, TOTH SZ, KOVACS D, KALMAN N, RADNAI B, DERES L, GALLYAS F, TOTH K, HALMOSI R. Mitochondrial protective effects of PARP-inhibition in hypertension-induced myocardial remodeling and in stressed cardiomyocytes. Life Sciences 268 Paper: 118936, 15 p. (2021)
Q1, IF: 6,78

MAGYAR K, DERES L, EROS K, **BRUSZT K**, SERESS L, HAMAR J, HIDEG K, BALOGH A, GALLYAS F, SUMEGI B, TOTH K, HALMOSI R. A quinazoline-derivate compound with PARP inhibitory effect suppresses hypertension-induced vascular alterations in spontaneously hypertensive rats. Biochimica et Biophysica Acta (BBA) 1842(7):935-944 (2014)
Q1, IF: 2,88

Published abstracts

BRUSZT K, HORVÁTH O, TAKÁCS-ÖRDÖG K, TÓTH SZ, VÁMOS E, JUHÁSZ K, TÓTH K, DERES L, HALMOSI R. A levoszimendan és aktív metabolitjának a mitokondrium működésére kifejtett hatásainak vizsgálata. CARDIOLOGIA HUNGARICA 54: Suppl. C Paper: C260 (2024)

BRUSZT K, HORVÁTH O, ÖRDÖG K, TÓTH SZ, VÁMOS E, GALLYAS F, TÓTH K, DERES L. Hagyományos és új típusú pozitív inotróp szerek hatása a mitokondriális légzés hatékonyságára. CARDIOLOGIA HUNGARICA 53: Suppl. A Paper: A279-A279 (2023)

HORVÁTH O, ÖRDÖG K, **BRUSZT K**, TÓTH SZ, DERES L, GALLYAS F, TÓTH K, SOÓS SZ, HALMOSI R. A BGP-15 kezelés hatása a szívfunkcióra bleomycin indukálta jobb szívfél elégtelenség modellben. CARDIOLOGIA HUNGARICA 53 : Suppl. A pp. A301-A301. (2023)

ÖRDÖG K, HORVÁTH O, TÓTH SZ, **BRUSZT K**, HABON T, KOVÁCS K, GALLYAS F, TÓTH K, DERES L, HALMOSI. A kolhicin hatásának vizsgálata pulmonális artériás hipertóniára patkány modellben. CARDIOLOGIA HUNGARICA 53 : Suppl. A pp. A303-A303. (2023)

BRUSZT K, HORVÁTH O, ÖRDÖG K, TÓTH SZ, FEKETE K, VÁMOS E, TÓTH K, DERES L, HALMOSI R. Dopamin és dobutamin hatása a mitokondriális légzés hatékonyságára szívizomsejtekben. CARDIOLOGIA HUNGARICA 52: Suppl. C: Paper: C253 (2022)

TÓTH SZ, ÖRDÖG K, HORVÁTH O, **BRUSZT K**, FEKETE K, GALLYAS F, TÓTH K, HALMOSI R, DERES L. OPA1 fehérje promóció hatása a mitokondriális dinamika folyamataira transzgén állatmodellben. CARDIOLOGIA HUNGARICA 52: Suppl. C: Paper: C261 (2022)

BRUSZT K, HORVÁTH O, ÖRDÖG K, TÓTH SZ, VÁMOS E, TÓTH K, DERES L, HALMOSI R. Mitokondriális légzés változásának vizsgálata dopamin és dobutamin hatására H9C2 sejttenyészetben. Magyar Haemorheologiai Társaság XXVIII., Magyar Mikrocirkulációs és Vaszkuláris Biológiai Társaság, Magyar Szabadgyök-Kutató Társaság, VII. Közös Kongresszusa Pécs, 2022. április 22-23. Programfüzet: 36. oldal (2022)

TÓTH SZ, ÖRDÖG K, HORVÁTH O, **BRUSZT K**, FEKETE K, GALLYAS F, TÓTH K, HALMOSI R, DERES L. OPA1 fehérje promóció kardiológiai hatásainak karakterizációja transzgén állatmodellben. Magyar Haemorheologiai Társaság XXVIII., Magyar Mikrocirkulációs és Vaszkuláris Biológiai Társaság, Magyar Szabadgyök-Kutató Társaság, VII. Közös Kongresszusa Pécs, 2022. április 22-23. Programfüzet: 35. oldal (2022)

ÖRDÖG K, HORVÁTH O, **BRUSZT K**, HABON T, KÁLAI T, DERES L, TÓTH K, HALMOSI R. PARP gátlás hatása oxidatív stresszben a mitokondriális biogenezisre in vitro szívizomsejt modellben. CARDIOLOGIA HUNGARICA 51: Supp. B Paper: B243-244 (2021)

DERES L, TÓTH SZ, **BRUSZT K**, ÖRDÖG K, HORVÁTH O, GALLYAS F, TÓTH K, HALMOSI R. OPA1 fehérje promóció kardiológiai hatásainak karakterizációja transzgén állatmodellben. CARDIOLOGIA HUNGARICA 51: Supp. B Paper: B274 (2021)

HORVÁTH O, ÖRDÖG K, **BRUSZT K**, DERES L, GALLYAS F, TÓTH K, HALMOSI R. A BGP-15 kezelés hatása a mitokondriális minőségkontroll folyamataira in vivo magasvérnyomás indukálta szívelégtelenség modellben. CARDIOLOGIA HUNGARICA 50: Supp. D Paper: 161 (2020)

HORVATH O, DERES L, ORDOG K, **BRUSZT K**, SUMEGI B, TOTH K, HALMOSI R. Role of BGP-15 treatment in hypertensive heart failure Progression and mitochondrial protection. EUROPEAN HEART JOURNAL 40: Suppl. 1 Paper: P5994 (2019)

HORVÁTH O, ÖRDÖG K, **BRUSZT K**, DERES L, SÜMEGI B, TOTH K, HALMOSI R. A BGP-15 kezelés hatása a mitokondriális dinamikára és funkcióra élő állat modellen és sejtkultúrában. CARDIOLOGIA HUNGARICA 49: Suppl. B Paper: B23 (2019)

ÖRDÖG K, HORVÁTH O, **BRUSZT K**, HALMOSI R, TOTH K, SÜMEGI B, DERES L. Az L-2286 kezelés hatása oxidatív stresszben a mitokondriális dinamikára és funkcióra in vitro kardiomioblaszt modellben. CARDIOLOGIA HUNGARICA 49: Suppl. B Paper: B14 (2019)

K MAGYAR, Z VAMOS, **K BRUSZT**, A BALOGH, T KALAI, K HIDEG, L SERESS, B SUMEGI, A KOLLER, R HALMOSI, K TOTH. Inhibition of Poly(ADP-ribose) polymeras ereduces hypertension induced vascular remodeling in spontaneous hypertensive rat model. Second international Symposium on Hypertension, november 18-21, 2010, Osijek, Croatia, Kidney and Blood Pressure Research 2010; 33: 425 (2010)

K BRUSZT, K MAGYAR, Z VAMOS, A BALOGH, T KÁLAI, K HIDEG, L SERESS, B SUMEGI, A KOLLER, R HALMOSI, K TOTH. Vasoprotective effect of a quinazoline-type Poly(ADP-Ribose)polymerase inhibitor against vascular remodeling in chronic hypertension. VI. International Symposium On Myocardial Cytoprotection, 7.9 October, 2010, Pécs, Hungary, Experimental and Clinical Cardiology, 2010; 5, 42 (2010)

K MAGYAR, **K BRUSZT**, Z VAMOS, I SOLTI, T KÁLAI, K HIDEG, L SERESS, B SUMEGI, A KOLLER, R HALMOSI, K TOTH. Vasoprotective effects of poly(ADP-ribose)polimerase inhibition in a spontaneously hypertensive rat model. VI. International Symposium On Myocardial Cytoprotection, 7.9 October, 2010, Pécs, Hungary, Experimental and Clinical Cardiology 2010; 5, 48 (2010)

K MAGYAR, Z VAMOS, **K BRUSZT**, I SOLTI, K HIDEG, B SUMEGI, A KOLLER, R HALMOSI, K TOTH. Vasoprotective effects of a novel PARP- inhibitor in spontaneously hypertensive rats. Congress of the European Society of Cardiology, 28 August - 01 September, 2010, Stockholm, Sweden EHJ, 31, Abstract Suppl., 84 (2010)

MAGYAR K, VÁMOS Z, **BRUSZT K**, SOLTI I, HIDEG K, KOLLER Á, SÜMEGI B, SERESS L, HALMOSI R. Poli(ADP-ribóz) polimeráz gátlásának vazoprotektív hatása spontán hipertenzív patkánymodellben. 40. Membrán-transzport konferencia, 2010. május 18-21., Sümeg. Absztrakt füzet 100. oldal (2010)

MAGYAR K, RIBA Á, **BRUSZT K**, BALOGH A, HIDEG K, SERESS L, SÜMEGI B, TÓTH K, HALMOSI R. Az L-2286 jelű PARP-gátló vegyület lehetséges szerepe a miokardialis őssejt regenerációban. CARDIOLOGIA HUNGARICA 42: Suppl. A Paper: A30 (2010)

MAGYAR K, VÁMOS Z, **BRUSZT K**, SOLTI I, CSÉPLŐ P, HIDEG K, SÜMEGI B, TÓTH K, HALMOSI R, KOLLER Á. Egy új PARP-gátló vazoprotekív hatása spontán hipertóniás patkányokban. CARDIOLOGIA HUNGARICA 40: Suppl. G Paper: G:45 (2010)